Journal of Solid Mechanics Vol. 15, No. 2 (2023) pp. 160-173
DOI: 10.22034/jsm.2023.1973962.1758

Research Paper

Closed-Form Formulation for Bending Analysis of Functionally Graded Thick Plates

M. Shaban[1,*], M.J. Khoshgoftar [2]

[1]*Mechanical Engineering Department, Bu-Ali Sina University, Hamadan, Iran*
[2]*Department of Mechanical Engineering, Faculty of Engineering, Arak University, Arak, Iran*

Received 17 February 2023; accepted 5 April 2023

ABSTRACT

Due to their continuous material variation and eliminating the mismatch stress field in the thickness direction, Functionally Graded Materials (FGMs) have found wide applications in aerospace and mechanical engineering. This article presents closed-form solution for thick functionally graded plate based on three-dimensional elasticity theory. To this end, first, the characteristic equation of FG plate is derived and general closed-form is obtained analytically. Both positive and negative discriminant of characteristic equation is considered and solved. The presented method is validated with finite element results by considering isotropic thick plate. Several parametric studies are carried out to investigate the effect of geometric and material parameters. The aim of this research is to present analytical solution form for thick FG plate and work out the problem of inconsistency for corresponding displacements field. The presented solution can be used to examine accuracy of various plate theories such as first-order, third order shear deformation theories and other equivalent plate theories.

Keywords: Functionally graded material; Bending analysis; Elasticity approach; Thick plate; Exact solution.

1 INTRODUCTION

FUNCTIONALLY Graded Materials (FGMs) can be defined as a composite type in which the mechanical properties varied gradually between two points. Due to the continuously varying material properties in space on the macroscopic scale, FGMs are usually superior to the conventional fiber-matrix materials in mechanical behavior, especially under thermal loads. Functionally graded materials reduce the mismatch between the material properties at the adjacent layers in layered composite that renders stress concentration between layers. FGMs are usually superior to the conventional fiber-matrix materials in mechanical behavior because of the continuously varying material properties. Due to their distinct properties, FGMs are widely used in aerospace and biomedical field. Numerous theories exist for modeling and analysis of functionally graded beams [1]–[4] and plates [5]–[8]. In these

*Corresponding author. Tel.: +98 9124786113.
E-mail address: m.shaban@basu.ac.ir (M.Shaban)

investigations, the displacement field is commonly simplified in the thickness direction due to relative smaller thickness compared to other dimensions. Compared to these theories, some researchers employed different solutions to obtain an analytical solution for three-dimensional (3D) stress analysis based on 3D elasticity theory for FGM thick plates. Swaminathan et al. [9] presented a brief review on the stress, vibration and buckling analysis of FGM plates including effects of variation of material properties through the thickness, type of load case, boundary conditions, edge ratio, side-to-thickness ratio and the effect of nonlinearity on the behavior of FGM plates. Three-dimensional elasticity solution for a rectangular laminated plate with pinned edges published with Pagano [10]. He assumed the exponential variation in the thickness direction and determined the unknown coefficients. Pagano's solution is extended by Pan [11] for functionally graded anisotropic elastic composite laminate. Li et al. obtained an elastic solution for a circular FGM plate subjected to pure bending [12] and transverse load [13]. They considered an arbitrary function in the thickness coordinate for elastic compliance coefficient. Zenkour [14] considered the effect of both transverse shear and normal deformations to solve the 3D elasticity equations for the bending analysis of simply-supported FGM plates. Also, He presented a trigonometric theory for thick exponentially graded plates and showed that the obtained displacements and stresses are more accurate when compared to the higher-order shear deformation plate theory. 3D analytical solutions have been derived for a transversely isotropic functionally graded circular plate subject to concentrated edge forces and couples by Liu et al. [15]. They used a displacement field solution that satisfies the 3D equilibrium equations and the traction boundary conditions on the top and bottom surfaces of the plate. Perturbation method is applied for a non-uniform pressurized functionally graded cylinder with variable thickness by Khoshgoftar et al. [16]. They used energy approach and first-order shear deformation theory for deriving governing equations. Also, a second-order theory as a higher-order theory is developed for axisymmetric thick shell by Khoshgoftar [17]. He applied a second-order polynomial function in thickness coordinate as non-linearity function for thick thickness. Omidi bidgoli et al. [18] studied bending behavior of a FG rotating cylindrical shell exposed to both pressure and surface shear stresses due to friction. They considered power law distribution for thermomechanical material properties and employed energy method and Euler equation for constitutive differential equations of the rotating shell. Kumari [19] developed a closed-form solution using extended Kantorovich method for a three-dimensional analytical solution for a functionally graded plate with longitudinally varying material properties. Lu et al [20] presented a semi-analytical 3-D elasticity solution for orthotropic multi-directional functionally graded plates using the differential quadrature method (DQM). They studied the effects of the material gradient for the in-plane variation in addition to the thickness direction, on the static response of multidirectional FGM plates. Habibi et al. [21] determined Stress Intensity Factor foe thick FG cylindrical vessel that have an internal semi-elliptical surface crack. They assumed that the FG material has exponentially varying properties and determined KI by using the BEM and FEM. Kardomateas et al [22] in their good paper presented three-dimensional elasticity solution for sandwich beams. They derived corresponding solution for the more complex case of positive discriminant of characteristic equations.

In this article, the closed-form solution is derived for thick functionally graded plate based on three-dimensional elasticity theory. The characteristic equation of FG plate is derived and solved analytically. Both positive and negative discriminant of characteristic equation is considered and solved. The coupled differential equations are solved for simply supported boundary condition by using Euler solution form. The aim of this research is to present analytical solution form for thick FG plate and work out the problem of inconsistency for corresponding displacements field. Furthermore, the solution form for isotropic thick plate as a special case of FG plate is provided. The corresponding stress field is derived for every solution form. In addition, the effect of some important parameters such as material index and thickness is investigated on the bending of the plate. The presented solution can be used to determine accuracy of various plate theories and numerical methods.

2 ELASTICITY SOLUTION

2.1 Functionally graded material

A thick rectangular flat plate made from FGM is considered in Cartesian coordinate (x,y,z) (Fig. 1).

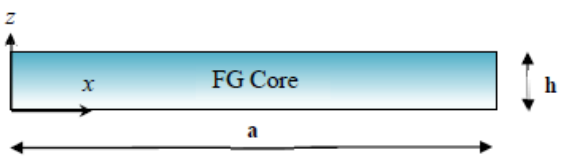

Fig.1
Schematic representation of functionally graded thick plate.

The Young modulus in the thickness direction varies in a smooth and continuous manner through exponential low:

$$E\left(z\right)=E_0\,\mathrm{e}^{\alpha z} \tag{1}$$

where E_0 is Young modulus of the plate at the bottom (metal rich). α is the FG index corresponding to exponential law which is usually positive real number. Based on the three-dimensional elasticity theory, the constitutive relations of elastic FG material can be written as [23]:

$$\{\vec{\sigma}\}=[C]\{\vec{\varepsilon}\} \tag{2}$$

where $\{\vec{\sigma}\}$ denote stress vector $\{\vec{\sigma}\}=\{\sigma_x \quad \sigma_y \quad \sigma_z \quad \tau_{yz} \quad \tau_{xz} \quad \tau_{xy}\}^T$, $\{\vec{\varepsilon}\}$ denote strain vector $\{\vec{\varepsilon}\}=\{\varepsilon_x \quad \varepsilon_y \quad \varepsilon_z \quad \gamma_{yz} \quad \gamma_{xz} \quad \gamma_{xy}\}^T$ and [*C*] is 6×6 matrix that represents the material constants and can be calculated in terms of Lamé constants λ and μ as follow [24]:

$$\begin{aligned} &C_{11}=C_{22}=C_{33}=\lambda+2\mu \\ &C_{12}=C_{13}=C_{23}=\lambda \\ &C_{44}=C_{55}=C_{66}=\mu \end{aligned} \tag{3}$$

And other C_{ij}s are zero. It is evident that Lamé constants are functions of *z*-coordinate:

$$\mu=\frac{E\left(z\right)}{2\left(1+\nu\right)},\ \lambda=\frac{\nu E\left(z\right)}{\left(1+\nu\right)\left(1-2\nu\right)} \tag{4}$$

The Poisson's ratio is considered to be constant [25]. Three equilibrium mechanical equations are

$$\begin{aligned} &\sigma_{x,x}+\tau_{xy,y}+\tau_{xz,z}=0, \\ &\tau_{xy,x}+\sigma_{y,y}+\tau_{yz,z}=0, \\ &\tau_{xz,x}+\tau_{yz,y}+\sigma_{z,z}=0. \end{aligned} \tag{5}$$

where $_{i,j}$ indicate the partial derivative with respect to *j*. The relationship between strain components and displacements are

$$\begin{aligned} &\varepsilon_x=u_{,x},\ \varepsilon_y=v_{,y},\ \varepsilon_z=w_{,z}, \\ &\gamma_{zy}=w_{,y}+v_{,z},\ \gamma_{zx}=w_{,x}+u_{,z},\ \gamma_{xy}=v_{,x}+u_{,y}. \end{aligned} \tag{6}$$

where *u, v* and *w* are the displacements of an arbitrary material point at the *x, y* and *z* direction, respectively. To present closed-form solution, simply supported boundary condition is considered as follow:

$$\begin{aligned} &v=0, w=0, \sigma_x=0, \quad \text{at } x=0,a \\ &u=0, w=0, \sigma_y=0, \quad \text{at } y=0,b \end{aligned} \tag{7}$$

By using separation of variables the following solutions for displacement components are assumed to satisfy the above boundary conditions;

$$
\begin{aligned}
u(x,y,z) &= \sum_{n=1}^{\infty}\sum_{m=}^{\infty} U_{nm}(z)\cos(px)\sin(qy),\\
v(x,y,z) &= \sum_{n=1}^{\infty}\sum_{m=}^{\infty} V_{nm}(z)\sin(px)\cos(qy),\\
w(x,y,z) &= \sum_{n=1}^{\infty}\sum_{m=}^{\infty} W_{nm}(z)\sin(px)\sin(qy).
\end{aligned}
\tag{8}
$$

where $p=\frac{n\pi}{a}$, $q=\frac{m\pi}{b}$ and $U_{nm}(z), V_{nm}(z), W_{nm}(z)$ are functions of z coordinate that should be determined. Substitution of relations (8) into Eqs. (6) and then considering constitutive Eq. (2) and by substitution of the results into Eqs. (5), one can obtain the following ordinary differential equations

$$
\begin{aligned}
&(1-2\nu)U''_{nm}(z)+(1-2\nu)\alpha U'_{nm}(z)+pW'_{nm}(z)+2(\nu-1)\left(p^2+q^2\right)U_{nm}(z)-pqV_{nm}(z)\\
&+(1-2\nu)\alpha p\,W_{nm}(z)=0,\\
&(1-2\nu)V''_{nm}(z)+(1-2\nu)\alpha V'_{nm}(z)+qW'_{nm}(z)+2(\nu-1)\left(p^2+q^2\right)V_{nm}(z)-pqU_{nm}(z)\\
&+(1-2\nu)\alpha q\,W_{nm}(z)=0,\\
&2(1-\nu)W''_{nm}(z)+2(1-\nu)\alpha W'_{nm}(z)-pU'_{nm}(z)-qV'_{nm}(z)-2\nu\alpha\left[pU_{nm}(z)+qV_{nm}(z)\right]\\
&+(2\nu-1)\left(p^2+q^2\right)W_{nm}(z)=0.
\end{aligned}
\tag{9}
$$

The above governing equations are coupled ordinary differential equations. To solve the mentioned equations, exponential form of solution is considered for any term of solution:

$$
\begin{aligned}
U_{nm}(z) &= Ue^{sz},\\
V_{nm}(z) &= Ve^{sz},\\
W_{nm}(z) &= We^{sz}.
\end{aligned}
\tag{10}
$$

By substituting Eqs. (10) into Eqs. (9), the following homogeneous algebraic equations are obtained:

$$
\begin{bmatrix}
S-2p^2-q^2 & -pq & p(\alpha+s-2\nu\alpha)\\
-pq & S-p^2-2q^2 & q(\alpha+s-2\nu\alpha)\\
-p(s+2\nu\alpha) & -q(s+2\nu\alpha) & s^2+\alpha s-p^2-q^2+S
\end{bmatrix}
\begin{bmatrix}U\\V\\W\end{bmatrix}=\vec{0}
\tag{11}
$$

where $S=(1-2\nu)\left(s^2+\alpha s\right)+2\nu\left(p^2+q^2\right)$. A nontrivial solution of homogeneous Eqs. (11) exists if the determinant of the coefficient matrix vanishes. Hence, the characteristic equation of the FG plate obtained by setting the determinant zero:

$$
\begin{aligned}
&\left(s^2+\alpha s-p^2-q^2\right)\left[s^4+2\alpha s^3+\left(\alpha^2-2p^2-2q^2\right)s^2-2\alpha\left(p^2+q^2\right)s\right.\\
&\left.+\left(p^2+q^2\right)\left[\left(p^2+q^2\right)+\nu\alpha^2/(1-\nu)\right]\right]=0
\end{aligned}
\tag{12}
$$

The characteristic equation is a sixth-order equation in terms of s. this equation can be separated to multiplication of a quadratic and quartic equation. The corresponding roots of the quadratic equation is obtained as:

$$s_{1,2} = -\frac{\alpha}{2} \pm \gamma_1 \tag{13}$$

where $\gamma_1 = \sqrt{\left(\frac{\alpha}{2}\right)^2 + p^2 + q^2}$ .These two roots are always real and distinct ones; The second equation is a quartic equation and cannot be solved directly. Let we consider $s = s' - \frac{\alpha}{2}$, thus the quartic characteristic equation can be written in term of s':

$$s'^4 - 2P s'^2 + P^2 + R = 0 \Rightarrow \left(s'^2 - P\right)^2 = -R \tag{14}$$

where $P = \gamma_1^2 = \frac{\alpha^2}{4} + p^2 + q^2$, $R = \frac{\nu}{1-\nu}\alpha^2\left(p^2 + q^2\right)$, which is a biquadratic equation in term of s'. The solution for s'^2 is

$$s'^2 = P \pm \sqrt{-R} \tag{15}$$

It should be noted that for usual engineering materials, the Poisson's ratio is smaller than 1; thus R is always positive and the obtained solutions in relation (15) are complex numbers. Thus we can rewrite the solution in form of Euler polar formula:

$$s'^2 = P \pm \sqrt{R}\, i = r e^{\pm i\theta},\ 0 < \theta < \pi/2 \tag{16}$$

where $r = \sqrt{P^2 + R}$, $\theta = \arctan\left(\frac{\sqrt{R}}{P}\right)$. By solving Eqs. (16) in polar form for s', the corresponding roots of the quartic equation is determined as follow:

$$s_{3,4} = -\frac{\alpha}{2} + \gamma_2 \pm i\gamma_3,\ s_{5,6} = -\frac{\alpha}{2} - \gamma_2 \pm i\gamma_3 \tag{17}$$

where $\gamma_2 = \sqrt{r}\cos\frac{\theta}{2}$, $\gamma_3 = \sqrt{r}\sin\frac{\theta}{2}$. By considering all the roots, the resultant solutions for displacement field can be written as follow:

$$\begin{aligned}
U(z) &= a_{u1}e^{s_1} + a_{u2}e^{s_2} + e^{-\alpha z/2}\left(a_{u3}e^{\gamma_2 z}\cos\gamma_3 z + a_{u4}e^{\gamma_2 z}\sin\gamma_3 z\right.\\
&\left. + a_{u5}e^{-\gamma_2 z}\cos\gamma_3 z + a_{u6}e^{-\gamma_2 z}\sin\gamma_3 z\right)\\
V(z) &= a_{v1}e^{s_1} + a_{v2}e^{s_2} + e^{-\alpha z/2}\left(a_{v3}e^{\gamma_2 z}\cos\gamma_3 z + a_{v4}e^{\gamma_2 z}\sin\gamma_3 z\right.\\
&\left. + a_{v5}e^{-\gamma_2 z}\cos\gamma_3 z + a_{v6}e^{-\gamma_2 z}\sin\gamma_3 z\right)\\
W(z) &= a_{w1}e^{s_1} + a_{w2}e^{s_2} + e^{-\alpha z/2}\left(a_{w3}e^{\gamma_2 z}\cos\gamma_3 z + a_{w4}e^{\gamma_2 z}\sin\gamma_3 z\right.\\
&\left. + a_{w5}e^{-\gamma_2 z}\cos\gamma_3 z + a_{w6}e^{-\gamma_2 z}\sin\gamma_3 z\right)
\end{aligned} \tag{18}$$

where a_{ij}, $i = u, v, w$, $j = 1\cdots 6$ are unknown coefficients that should be determined. The above relations can be written in polar form as follow:

$$
\begin{aligned}
U(z) &= e^{-\alpha z/2}\left[a_{u1}e^{\gamma_1 z} + a_{u2}e^{-\gamma_1 z} + a_{u3}e^{\mu_1 z} + a_{u4}e^{\bar{\mu}_1 z} + a_{u5}e^{\mu_2 z} + a_{u6}e^{\bar{\mu}_2 z}\right)\\
V(z) &= e^{-\alpha z/2}\left[a_{v1}e^{\gamma_1 z} + a_{v2}e^{-\gamma_1 z} + a_{v3}e^{\mu_1 z} + a_{v4}e^{\bar{\mu}_1 z} + a_{v5}e^{\mu_2 z} + a_{v6}e^{\bar{\mu}_2 z}\right)\\
W(z) &= e^{-\alpha z/2}\left[a_{w1}e^{\gamma_1 z} + a_{w2}e^{-\gamma_1 z} + a_{w3}e^{\mu_1 z} + a_{w4}e^{\bar{\mu}_1 z} + a_{w5}e^{\mu_2 z} + a_{w6}e^{\bar{\mu}_2 z}\right)
\end{aligned}
\tag{19}
$$

where $\mu_1 = \gamma_2 + i\gamma_3$, $\mu_2 = -\gamma_2 + i\gamma_3$ and $\bar{\mu}_i$ is complex conjugate of μ_i. Note that the coefficients a_{ij}, in relations (18) is differ from relations (19) and depends to the selection of solution form. Of the 18 coefficients a_{ij}, only six of them are independent and other dependent coefficients can be obtained in terms of independent ones. For the first two displacement terms $a_{u1}, a_{u2}, a_{v1}, a_{v2}, a_{w1}, a_{w2}$ by considering $s_{1,2}$ in Eq. (13) and replacing the solution in matrix Eq. (11) we obtain that:

$$
\begin{bmatrix}
-p^2 & -pq & -p\left(2\alpha\nu - \alpha/2 \mp \gamma_1\right)\\
-pq & -q^2 & -q\left(2\alpha\nu - \alpha/2 \mp \gamma_1\right)\\
-p & -q & \left(p^2+q^2\right)\Big/\left(2\alpha\nu - \alpha/2 \pm \gamma_1\right)
\end{bmatrix}
\begin{bmatrix} a_{u_i}\\ a_{v_i}\\ a_{w_i}\end{bmatrix} = \vec{0}
\qquad i = 1,2
\tag{20}
$$

The first two equations in above matrix are same and so the determinant of coefficient is zero. But on the other hand, by considering one of first two equations with the last equation, we found that the system of matrix equation is inconsistent. The only solution that leads to consistent solution is $\nu = 0.5$ i.e., rigid body. By substituting the corresponding terms of solution consist of $a_{u1}, a_{u2}, a_{v1}, a_{v2}, a_{w1}, a_{w2}$ in governing equation the relation between coefficients is obtained as:

$$
a_{v1} = -\frac{p}{q}a_{u1}, \quad a_{v2} = -\frac{p}{q}a_{u2}, a_{w1} = a_{w2} = 0
\tag{21}
$$

By using the constitutive relations, stress components will be obtained

$$
\begin{aligned}
&\sigma_{xx}(x,y,z) = -\sigma_{yy}(x,y,z) = -C^*\sin(px)\sin(qy)\,p\,a_{ui},\ \sigma_{zz}(x,y,z) = 0\\
&\tau_{yz}(x,y,z) = C^*\sin(px)\cos(qy)\left(\frac{-p}{2q}s_i\right)a_{ui}\\
&\tau_{xz}(x,y,z) = C^*\cos(px)\sin(qy)\left(\frac{s_i}{2}\right)a_{ui}\\
&\tau_{xy}(x,y,z) = C^*\cos(px)\sin(qy)\left[\frac{1}{2}\left(q - \frac{p^2}{q}\right)\right]a_{ui}
\end{aligned}
\tag{22}
$$

where $C^* = \dfrac{e^{s_i z + \alpha\left(z - z_0\right)}E_0}{(\nu+1)}$ and i=1,2. By considering the second two displacement terms for $s_{3,4}$ in Eq. (17), the $a_{u3}, a_{u4}, a_{v3}, a_{v4}, a_{w3}, a_{w4}$ are determined:

$$
\begin{aligned}
&a_{v3} = (q/p)a_{u3},\ a_{v4} = (q/p)a_{u4}\\
&a_{u3} = \xi_{33}a_{w3} + \xi_{34}a_{w4},\ \ a_{u4} = \xi_{43}a_{w3} + \xi_{44}a_{w4}
\end{aligned}
\tag{23}
$$

where

$$\xi_{33}=\xi_{44}=\frac{\left[r_0\left(p^2+q^2\right)+r_2\gamma_3\right]}{\xi^{**}}p$$
$$\xi_{34}=-\xi_{43}=-\frac{\left[-\gamma_3\left(p^2+q^2\right)+r_0 r_2\right]}{\xi^{**}}p$$
$$\xi^{**}=\left(p^2+q^2\right)^2+R\left(1-2\nu\right)^2$$

And $r_0=\alpha/2+\gamma_2-2\alpha\nu,\ r_2=\left(2\nu-1\right)\sqrt{R}$. The corresponding stresses can be obtained as follow:

$$\sigma_{xx}\left(x,y,z\right)=C^{**}\sin\left(px\right)\sin\left(qy\right)\left[\varsigma_{13}^{**}\cos\gamma_3 z+\varsigma_{14}^{**}\sin\gamma_3 z\right]$$
$$\varsigma_{13}^{**}=-p\left(1-\nu\right)a_{\mathrm{u}3}-\nu q\,a_{\mathrm{v}3}+\nu\left(\gamma_2-\frac{\alpha}{2}\right)a_{\mathrm{w}3}+\nu\gamma_3 a_{\mathrm{w}4},$$
$$\varsigma_{14}^{**}=-p\left(1-\nu\right)a_{\mathrm{u}4}-\nu q\,a_{\mathrm{v}4}-\nu\gamma_3 a_{\mathrm{w}3}+\nu\left(\gamma_2-\frac{\alpha}{2}\right)a_{\mathrm{w}4}$$
$$\sigma_{yy}\left(x,y,z\right)=C^{**}\sin\left(px\right)\sin\left(qy\right)\left[\varsigma_{23}^{**}\cos\gamma_3 z+\varsigma_{24}^{**}\sin\gamma_3 z\right]$$
$$\varsigma_{23}^{**}=-\nu p\,a_{\mathrm{u}3}-\left(1-\nu\right)qa_{\mathrm{v}3}+\left(\gamma_2-\frac{\alpha}{2}\right)\nu a_{\mathrm{w}3}+\nu\gamma_3 a_{\mathrm{w}4},$$
$$\varsigma_{24}^{**}=-\nu p\,a_{\mathrm{u}4}-\left(1-\nu\right)q\,a_{\mathrm{v}4}-\nu\gamma_3 a_{\mathrm{w}3}+\left(\gamma_2-\frac{\alpha}{2}\right)\nu a_{\mathrm{w}4}$$
$$\sigma_{zz}\left(x,y,z\right)=C^{**}\sin\left(px\right)\sin\left(qy\right)\left[\varsigma_{33}^{**}\cos\gamma_3 z+\varsigma_{34}^{**}\sin\gamma_3 z\right]$$
$$\varsigma_{33}^{**}=\left(-\nu p\right)a_{\mathrm{u}3}+\left(-\nu q\right)a_{\mathrm{v}3}+\left(\gamma_2-\nu\gamma_2-\frac{\alpha}{2}+\frac{\alpha\nu}{2}\right)a_{\mathrm{w}3}+\left(1-\nu\right)\gamma_3 a_{\mathrm{w}4},$$
$$\varsigma_{34}^{**}=\left(-\nu p\right)a_{\mathrm{u}4}+\left(-\nu q\right)a_{\mathrm{v}4}-\left(1-\nu\right)\gamma_1 a_{\mathrm{w}3}+\left(\gamma_2-\nu\gamma_2-\frac{\alpha}{2}+\frac{\alpha\nu}{2}\right)a_{\mathrm{w}4} \tag{24}$$
$$\tau_{yz}\left(x,y,z\right)=2C^{**}\sin\left(px\right)\cos\left(qy\right)\left[\varsigma_{43}\cos\gamma_3 z+\varsigma_{44}\sin\gamma_3 z\right]$$
$$\varsigma_{43}=\frac{\left(\alpha-2\gamma_2\right)\left(2\nu-1\right)}{2}a_{\mathrm{v}3}-\gamma_3\left(2\nu-1\right)a_{\mathrm{v}4}-q\left(2\nu-1\right)a_{\mathrm{w}3},$$
$$\varsigma_{44}=\gamma_3\left(2\nu-1\right)a_{\mathrm{v}3}+\frac{\left(\alpha-2\gamma_2\right)\left(2\nu-1\right)}{2}a_{\mathrm{v}4}-q\left(2\nu-1\right)a_{\mathrm{w}4}$$
$$\tau_{xz}\left(x,y,z\right)=2C^{**}\sin\left(px\right)\cos\left(qy\right)\left[\varsigma_{53}\cos\gamma_3 z+\varsigma_{54}\sin\gamma_3 z\right]$$
$$\varsigma_{53}=\frac{\left(\alpha-2\gamma_2\right)\left(2\nu-1\right)}{2}a_{\mathrm{u}3}-\gamma_3\left(2\nu-1\right)a_{\mathrm{u}4}-p\left(2\nu-1\right)a_{\mathrm{w}3},$$
$$\varsigma_{54}=\gamma_3\left(2\nu-1\right)a_{\mathrm{u}3}+\frac{\left(\alpha-2\gamma_2\right)\left(2\nu-1\right)}{2}a_{\mathrm{u}4}-p\left(2\nu-1\right)a_{\mathrm{w}4}$$
$$\tau_{xy}\left(x,y,z\right)=2C^{**}\cos\left(px\right)\cos\left(qy\right)\left[\varsigma_{63}\cos\gamma_3 z+\varsigma_{64}\sin\gamma_3 z\right]$$
$$\varsigma_{63}=-q\left(2\nu-1\right)a_{\mathrm{u}3}-p\left(2\nu-1\right)a_{\mathrm{v}3},$$
$$\varsigma_{64}=-q\left(2\nu-1\right)a_{\mathrm{u}4}-p\left(2\nu-1\right)a_{\mathrm{v}4}$$

where $C^{**}=e^{-\frac{\alpha z}{2}+\gamma_2 z}\ \lambda/\nu$. Other remaining coefficients a_{ij} , $i=u,v,w$, $j=5,6$ obtained in similar manner by replacing γ_2 with $-\gamma_2$.

2.2 Isotropic material

Thick rectangular plate made of isotropic material is considered in this section. In fact, this case is a special case of FG material by setting α=0. But the solution form is changed. By vanishing parameter α from Eqs. (9) and substituting the solution form (10) in this equation, the following homogeneous matrix equation are obtained:

$$\begin{bmatrix} S-p^2 & -pq & ps \\ -pq & S-q^2 & qs \\ -ps & -qs & S+s^2 \end{bmatrix} \begin{bmatrix} U \\ V \\ W \end{bmatrix} = \vec{0} \qquad (25)$$
$$S = (1-2\nu)\left(s^2-p^2-q^2\right)$$

where $S = (1-2\nu)\left(s^2-p^2-q^2\right)$. Following same procedure described in previous section, the characteristic equation is determined as:

$$\left(s^2-p^2-q^2\right)^3 = 0 \qquad (26)$$

where is sixth-order equation and has real plus-minus root:

$$s_{1,2} = \pm\sqrt{\left(p^2+q^2\right)} = \pm\gamma_1 \qquad (27)$$

Corresponding to these two repeated real roots, the displacement functions are:

$$\begin{aligned} U(z) &= a_{u1}\cosh\gamma_1 z + a_{u2}\sinh\gamma_1 z + a_{u3} z\cosh\gamma_1 z + a_{u4} z\sinh\gamma_1 z + a_{u5} z^2\cosh\gamma_1 z + a_{u6} z^2\sinh\gamma_1 z \\ V(z) &= a_{v1}\cosh\gamma_1 z + a_{v2}\sinh\gamma_1 z + a_{v3} z\cosh\gamma_1 z + a_{v4} z\sinh\gamma_1 z + a_{v5} z^2\cosh\gamma_1 z + a_{v6} z^2\sinh\gamma_1 z \\ W(z) &= a_{w1}\cosh\gamma_1 z + a_{w2}\sinh\gamma_1 z + a_{w3} z\cosh\gamma_1 z + a_{w4} z\sinh\gamma_1 z + a_{w5} z^2\cosh\gamma_1 z + a_{w6} z^2\sinh\gamma_1 z \end{aligned} \qquad (28)$$

Of the unknown coefficients a_{ij}, $i = u,v,w$, $j = 1\cdots 6$ only six of them are independent and because the characteristic equation has repeated roots, all the displacement terms in the above relations should be considered. To determine the unknown independent coefficients, the relations (27) substituted in governing Eqs. (5). Solving the obtain equations and after some manipulation the following results can be obtained:

$$\begin{aligned} a_{v1} &= \frac{1}{q}\left[-pa_{u1} + \gamma_1 a_{w2} + (-4\nu+3)a_{w3}\right], \\ a_{v2} &= \frac{1}{q}\left[-pa_{u2} + \gamma_1 a_{w1} + (-4\nu+3)a_{w4}\right], \\ a_{u3} &= \frac{p\,\gamma_1}{p^2+q^2}a_{w4},\ a_{v3} = \frac{q\,\gamma_1}{p^2+q^2}a_{w4} \\ a_{u4} &= \frac{p\,\gamma_1}{p^2+q^2}a_{w3},\ a_{v4} = \frac{q\,\gamma_1}{p^2+q^2}a_{w3} \\ a_{ij} &= 0,\ i = u,v,w,\ j = 5,6 \end{aligned} \qquad (29)$$

where $a_{w1}, a_{w2}, a_{w3}, a_{w4}, a_{u1}, a_{u2}$ are independent coefficients. Constituting the relations (27) into constitutive Eqs. (2), the stress components can be obtained as follow:

$$\sigma_{xx}\left(x,y,z\right)=C^{*}\sin\left(px\right)\sin\left(qy\right)\left[\varsigma_{11}\cosh\gamma_1 z+\varsigma_{12}\sinh\gamma_1 z\right]$$
$$\varsigma_{11}=pa_{\mathrm{u1}}+2\nu a_{\mathrm{w3}}+p^2 z\,a_{\mathrm{w4}},\ \varsigma_{12}=pa_{\mathrm{u2}}+p^2 z\,a_{\mathrm{w3}}+2\nu a_{\mathrm{w4}}$$
$$\sigma_{yy}\left(x,y,z\right)=C^{*}\sin\left(px\right)\sin\left(qy\right)\left[\varsigma_{21}\cosh\gamma_1 z+\varsigma_{22}\sinh\gamma_1 z\right]$$
$$\varsigma_{21}=-pa_{\mathrm{u1}}+\gamma_1 a_{\mathrm{w2}}-\left(2\nu-3\right)a_{\mathrm{w3}}+q^2 z\,a_{\mathrm{w4}},\ \varsigma_{22}=-pa_{\mathrm{u2}}+\gamma_1 a_{\mathrm{w1}}+q^2 z\,a_{\mathrm{w3}}-\left(2\nu-3\right)a_{\mathrm{w4}}$$
$$\sigma_{zz}\left(x,y,z\right)=C^{*}\sin\left(px\right)\sin\left(qy\right)\left[\varsigma_{31}\cosh\gamma_1 z+\varsigma_{32}\sinh\gamma_1 z\right]$$
$$\varsigma_{31}=-\gamma_1 a_{\mathrm{w2}}+\left(2\nu-1\right)a_{\mathrm{w3}}-z\,\gamma_1 a_{\mathrm{w4}},\ \varsigma_{32}=-\gamma_1 a_{\mathrm{w1}}-z\,\gamma_1 a_{\mathrm{w3}}+\left(2\nu-1\right)a_{\mathrm{w4}}$$
$$\tau_{xz}\left(x,y,z\right)=2C^{*}\cos\left(px\right)\sin\left(qy\right)\left[\varsigma_{51}\cosh\gamma_1 z+\varsigma_{52}\sinh\gamma_1 z\right]$$
$$\varsigma_{51}=-\gamma_1 a_{\mathrm{u2}}-pa_{\mathrm{w1}}-2pz\,a_{\mathrm{w3}}-pa_{\mathrm{w4}},\ \varsigma_{52}=-\gamma_1 a_{\mathrm{u1}}-pa_{\mathrm{w2}}-pa_{\mathrm{w3}}-2pz\,a_{\mathrm{w4}}$$
$$\tau_{yz}\left(x,y,z\right)=2C^{*}\sin\left(px\right)\cos\left(qy\right)\left[\varsigma_{41}\cosh\gamma_1 z+\varsigma_{42}\sinh\gamma_1 z\right] \tag{30}$$
$$\varsigma_{41}=\frac{1}{q}\left\{\gamma_1 p\,a_{\mathrm{u2}}-\left(q^2+\gamma_1^2\right)a_{\mathrm{w1}}-2q^2 z\,a_{\mathrm{w3}}-\left[4\left(1-\nu\right)\gamma_1-p^2/\gamma_1\right]a_{\mathrm{w4}}\right\},$$
$$\varsigma_{42}=\frac{1}{q}\left\{\gamma_1 p\,a_{\mathrm{u1}}-\left(q^2+\gamma_1^2\right)a_{\mathrm{w2}}-\left[4\left(1-\nu\right)\gamma_1-p^2/\gamma_1\right]a_{\mathrm{w3}}-2q^2 z\,a_{\mathrm{w4}}\right\}$$
$$\tau_{xy}\left(x,y,z\right)=2C^{*}\cos\left(px\right)\cos\left(qy\right)\left[\varsigma_{61}\cosh\gamma_1 z+\varsigma_{62}\sinh\gamma_1 z\right]$$
$$\varsigma_{61}=\frac{1}{q}\left[\left(p^2-q^2\right)a_{\mathrm{u1}}-\gamma_1 p\,a_{\mathrm{w2}}+p\left(4\nu-3\right)a_{\mathrm{w3}}-\frac{2pq^2 z}{\gamma_1}a_{\mathrm{w4}}\right]$$
$$\varsigma_{62}=\frac{1}{q}\left[\left(p^2-q^2\right)a_{\mathrm{u2}}-\gamma_1 p\,a_{\mathrm{w1}}-\frac{2pq^2 z}{\gamma_1}a_{\mathrm{w3}}+p\left(4\nu-3\right)a_{\mathrm{w4}}\right]$$

where $C^{*}=-\dfrac{E_0}{\nu+1}$.

2.3 Boundary conditions

To calculate the unknown independent coefficients and complete the solution, six boundary conditions should be considered. These conditions are obtained by implementing the consistent top and bottom surface conditions as follow:

1. The bottom surface is traction free so $\sigma_{zz}=0,\ \tau_{xz}=0,\ \tau_{yz}=0$.
2. The top surface is exposed to only external transverse loading, so $\sigma_{zz}=Q\left(x,y,z\right)$ and $\tau_{xz}=0,\ \tau_{yz}=0$.

Considering the above boundary condition, all the coefficients are calculated and the solution will be completed.

3 NUMERICAL RESULTS AND DISCUSSION

In this article, first comparison study is provided and then parametric study is provided to investigate the bending behavior of thick plate based on elasticity theory.

The presented method is compared with Pagano [10] solution for isotropic plate and it was consistent with his presented solution (Table 1). As a first example, the accuracy of the presented method is examined by comparing the displacement and stress components of thick plate with those of the finite element (FE). It is assumed that the plate made of aluminum with E=70 *GPa* and v=0.3. Furthermore, the plate is square and a=0.1 *m*, h= 0.02 *m*. The upper surface is exposed to $Q\left(x,y,z\right)=q_0\sin\left(\dfrac{\pi x}{a}\right)\sin\left(\dfrac{\pi y}{b}\right)$ and q_0=-1*Pa*. The FE results are extracted from ABAQUS software with element type C3D8R which is three-dimensional element with 8-nodes. The distribution of displacements u and w are plotted in Fig. 2 for both analytical and FE results. u is plotted at x=0,y=b/2 and w is

plotted at $x=a/2$, $y=b/2$. Due to symmetry of loading the in-plane displacements u and v are equal. The out-of-plane stresses σ_{zz} , τ_{xz} are plotted in Fig. 2(b). The in-plane stresses σ_{xx} , τ_{xy} are plotted in Fig. 2(c). As one can see, the results are in accordance with considered boundary conditions in section 2.3. Very good agreement can be observed between results. In another example, FG plate with E_m=220 *GPa* and E_c=380 *GPa* is considered. The plate is divided into 32 sublayers and each sublayer is considered to has average Young modulus corresponding to middle coordinate of it (Fig. 3). Again good agreement is seen between results in Table 2. In the next example a thick FG plate is considered with top face Young modulus E_c=380*GPa*. Different values for the bottom modulus are considered, namely E_m=70, 150 and 230 *GPa*. The Poisson's ratio is 0.3. The geometric dimensions are same as the first example. Table 3 provide roots of characteristic equation for mentioned FG plate.

Table 1
Comparison of displacements for isotropic plate with Pagano [10] results.

$\frac{a}{h}$	$\bar{U}\left(0,\frac{b}{2},\frac{1}{2}\right)=\bar{V}\left(\frac{a}{2},0,\frac{1}{2}\right)$		$\bar{W}\left(\frac{a}{2},\frac{b}{2},1\right)$	
	Present	Ref. [10]	Present	Ref. [10]
2	5.01×10^{-12}	4.95×10^{-12}	-1.91×10^{-11}	-1.74×10^{-11}
4	4.12×10^{-11}	3.88×10^{-11}	-1.52×10^{-10}	-1.33×10^{-10}
10	6.45×10^{-10}	6.24×10^{-10}	-4.34×10^{-9}	-4.17×10^{-9}
20	5.51×10^{-9}	5.02×10^{-9}	-6.57×10^{-8}	-6.47×10^{-8}
50	8.02×10^{-8}	7.86×10^{-8}	-3.08×10^{-6}	-2.51×10^{-6}

Table 2
Comparison of displacements of FG plate with FE results.

	u_{max}	w_{max}
w (analytical)	3.0852×10^{-13}	1.764×10^{-12}
w (abaqus)	3.412×10^{-13}	1.187×10^{-12}

Table 3
The roots of characteristic equation for FG thick plate with different values of E_m (a=0.1*m*, h=0.02*m*, q_0=-1*Pa*)

E_m (*GPa*)	α	γ_1	γ_2	γ_3
70	84.58	61.3394	64.2572	19.1431
130	53.63	51.8943	53.8757	14.4769
190	34.66	47.6886	48.7945	10.3293
250	20.94	45.6453	46.1202	6.6014
310	10.18	44.7194	44.8412	3.3015

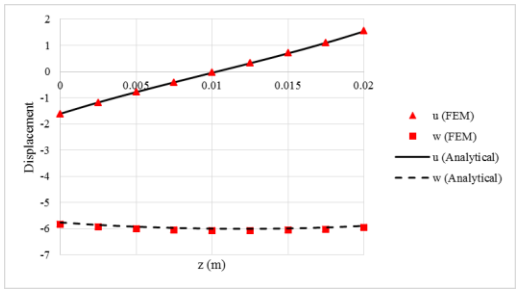

(a)

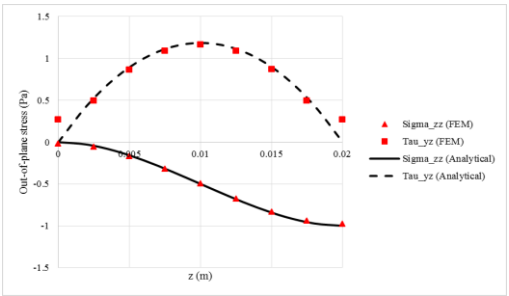

(b)

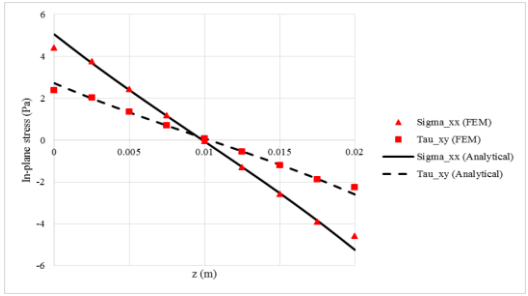

(c)

Fig.2
Comparison of displacements and stresses obtained by the present method with FE results.

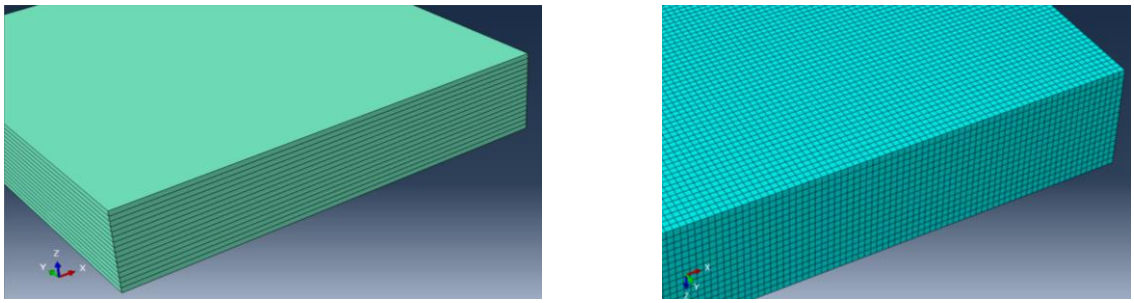

(a) (b)

Fig.3
Finite element model of thick FG plate.

Fig. 4(a) shows the distribution of Young modulus in the dimensionless thickness direction $\bar{z}$ ($\bar{z} = z/h$). In Figs. 4(b-g) dimensionless displacement components $\bar{U}$, $\bar{W}$ and stress components $\bar{\sigma}_{zz}$, $\bar{\tau}_{xz}$, $\bar{\tau}_{xy}$, $\bar{\sigma}_{xx}$ are plotted. It should be noted that the in-plane displacements and also in-plane stresses are equal due to transversely isotropic properties of FG plate.

As shown in Fig. 4(b-c), by increasing the Young modulus of bottom surface, the displacements reduced. Furthermore, the in-plane displacement cannot be neglected compared to transverse displacement. It can be concluded that increasing the E_m make the plate more stiff and therefore smaller displacements are obtained. In Fig. 4(d), variation of normal stress $\bar{\sigma}_{zz}$ through the thickness is plotted. As can be seen, normal stress is satisfied boundary conditions that should be zero and unit in bottom and top surface, respectively. Variation of $\bar{\tau}_{xz}$ is plotted in Fig. 4(e). It is evident that dimensionless transverse stress at the bottom and top surfaces is zero that satisfied external boundary conditions. According to Fig. 4(f-g), one can see that by increasing E_m the in-plane $\bar{\sigma}_{xx}$ decreased contrary to in-plane shear stress $\bar{\tau}_{xy}$. However nonlinear variation is evident especially for lower values of E_m.

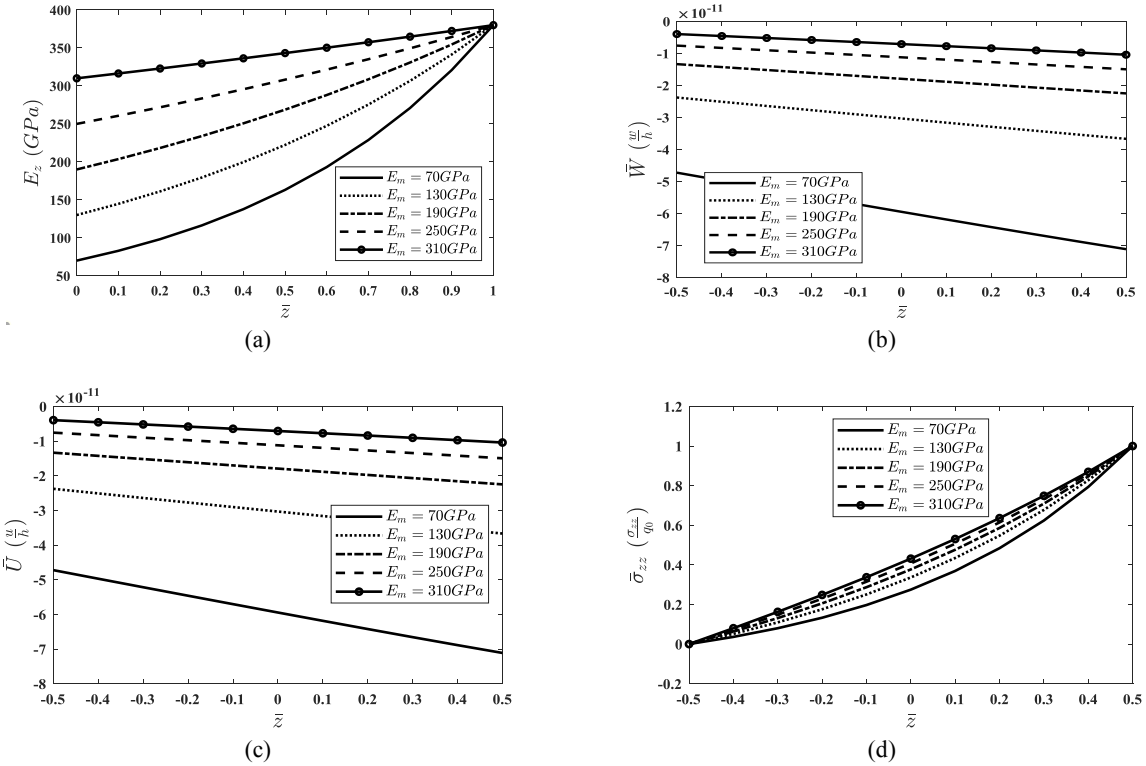

(a) (b)

(c) (d)

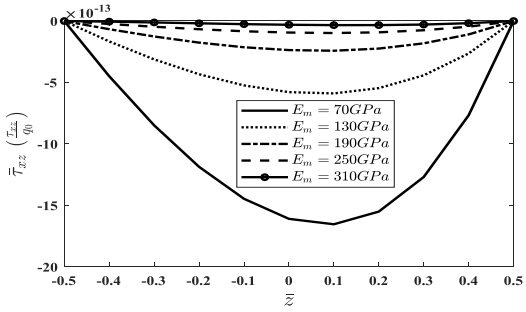

(e)

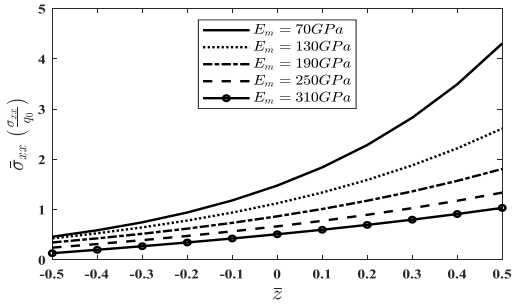

(f)

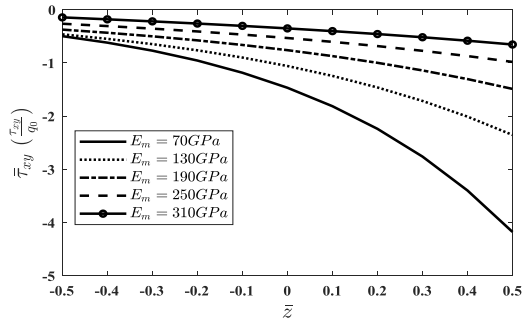

(g)

Fig.4
Variation of displacement and stress components of FG thick plate along *z*-direction for different values of E_m.

In the next example, the effect of thickness on the bending behavior of FG thick plate is considered. In this example it is assumed that Young modulus of top and bottom face is constant, thus the exponential FG index can be obtained by using the relation $\alpha=(1/h)Ln(E_c/E_m)$. Table 4 shows the roots of characteristic equation for four thickness, that is h=10, 15, 20 and 25 *mm*. As shown in Fig. 5(a), when the plate is thinner the transverse deflection increased. Although the thickness increased in equal-step manner, but the $\bar{W}$ has no equal-step increase.

The $\bar{\sigma}_{zz}$ is not affected significantly by changing thickness of FG plate as shown in Fig. 5(b). According to Figs. 5(c-d), the absolute value of in-plane stresses $\bar{\sigma}_{xx}$, $\bar{\tau}_{xy}$ and out-of-plane stress $\bar{\tau}_{xz}$ has an increase when the plate becomes thicker. As can be seen in these figures, increasing the thickness leads to smaller and smoother variation of stresses.

Table 4
Roots of characteristic equation for FG thick plate with different values of thickness *(a=0.1m, E_m =70GPa, E_c =380GPa, q_0=-1Pa)*

h (mm)	*α*	*γ_1*	*γ_2*	*γ_3*
25	67.67	55.8447	58.3368	16.8687
20	84.58	61.3394	64.2572	19.1431
15	112.78	71.7890	75.0422	21.8558
10	169.17	95.5423	98.7378	24.9161

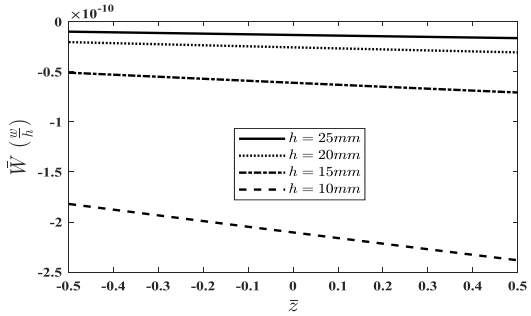

(a)

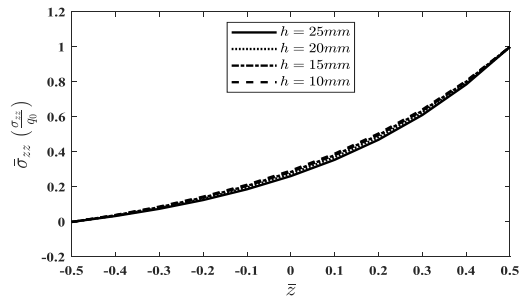

(b)

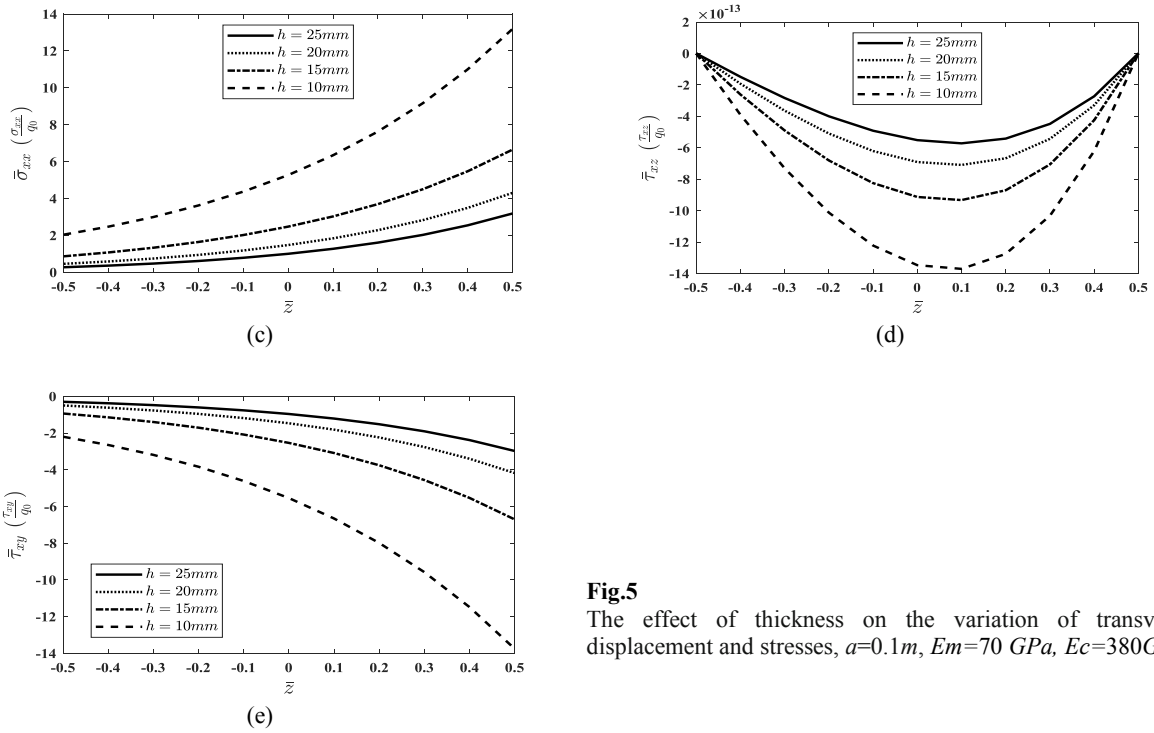

Fig.5
The effect of thickness on the variation of transverse displacement and stresses, a=0.1m, Em=70 *GPa, Ec*=380*GPa.*

4 CONCLUSION

In this study, exact solution have been proposed for bending analysis of thick functionally graded/isotropic plate. By considering three dimensional governing equations, the characteristic equation of FG plate is derived. The characteristic equation is separated to multiplication of a quadratic and quartic equation. Analytical solution for quartic equation is presented by means of complex form solution. Then real-value and complex form of solution are presented for ordinary differential equation based on Euler solution. A critical study is carried out to obtain unknown coefficient of real parts. Other coefficients are derived analytically by using dependency of equations. By applying the external boundary conditions, all six independent coefficients are calculated. The presented solution is provided for isotropic plate and validated by finite element results. Finally parametric studies are carried out to study the effect of geometrical and material parameters.

REFERENCES

[1] Ghorbanpour-Arani A. H., Rastgoo A., Sharafi M. M., Kolahchi R., Ghorbanpour Arani A., 2016, Nonlocal viscoelasticity based vibration of double viscoelastic piezoelectric nanobeam systems, *Meccanica* **51**(1): 25-40.

[2] Ghorbanpour-Arani A. H., Rastgoo A., Hafizi Bidgoli A., Kolahchi R., Ghorbanpour Arani A., 2017, Wave propagation of coupled double-DWBNNTs conveying fluid-systems using different nonlocal surface piezoelasticity theories, *Mechanics of Advanced Materials and Structures* **24**(14): 1159-1179.

[3] Ghorbanpour Arani A., Jamali M., Ghorbanpour-Arani A. H., Kolahchi R., Mosayyebi M., 2017, Electro-magneto wave propagation analysis of viscoelastic sandwich nanoplates considering surface effects, *Proceedings of the Institution of Mechanical Engineers Part C, Journal of Mechanical Engineering Science* **231**(2): 387-403.

[4] Ghorbanpour-Arani A. H., Abdollahian M., Ghorbanpour Arani A., 2020, Nonlinear dynamic analysis of temperature-dependent functionally graded magnetostrictive sandwich nanobeams using different beam theories, *Journal of the Brazilian Society of Mechanical Sciences and Engineering* **42**(6): 314.

[5] Shaban M., Alipour M. M., 2011, Semi-analytical solution for free vibration of thick functionally graded plates rested on elastic foundation with elastically restrained edge*, Acta Mechanica Solida Sinica* **24**(4): 340-354.

[6] Alipour M. M., Shariyat M., Shaban M., 2010, A semi-analytical solution for free vibration of variable thickness two-directional-functionally graded plates on elastic foundations, *International Journal of Mechanics and Materials in Design* **6**(4): 293-304.

[7] Shaban M., Mazaheri H., 2021, Bending analysis of five-layer curved functionally graded sandwich panel in magnetic field: closed-form solution, *Applied Mathematics and Mechanics* **42**(2): 251-274.
[8] Alipour M. M., Shariyat M., Shaban M., 2020, Free vibration analysis of bidirectional functionally graded conical/cylindrical shells and annular plates on nonlinear elastic foundations, based on a unified differential transform analytical formulation, *Journal of Solid Mechanics* **12**(2): 385-400.
[9] Swaminathan K., Naveenkumar D. T., Zenkour A. M., Carrera E., 2015, Stress, vibration and buckling analyses of FGM plates-A state-of-the-art review, *Composite Structures* **120**: 10-31.
[10] Pagano N. J., 1970, Exact solutions for rectangular bidirectional composites and sandwich plates, *Journal of Composite Materials* **4**(1): 20-34.
[11] Pan E., 2003, Exact solution for functionally graded anisotropic elastic composite laminates, *Journal of Composite Materials* **37**(21): 1903-1920.
[12] Li X. Y., Ding H. J., Chen W. Q., 2006, Pure bending of simply supported circular plate of transversely isotropic functionally graded material, *Journal of Zheijang University Science* **7**(8): 1324-1328.
[13] Li X. Y., Ding H. J., Chen W. Q., 2008, Elasticity solutions for a transversely isotropic functionally graded circular plate subject to an axisymmetric transverse load qrk, *International Journal of Solids and Structures* **45**(1): 191-210.
[14] Zenkour A. M., 2007, Benchmark trigonometric and 3-D elasticity solutions for an exponentially graded thick rectangular plate, *Archive of Applied Mechanics* **77**(4): 197-214.
[15] Liu N. W., Sun Y. L., Chen W. Q., Yang B., Zhu J., 2019, 3D elasticity solutions for stress field analysis of FGM circular plates subject to concentrated edge forces and couples, *Acta Mechanica* **230**(8): 2655-2668.
[16] Khoshgoftar M. J., Mirzaali M. J., Rahimi G. H., 2015, Thermoelastic analysis of non-uniform pressurized functionally graded cylinder with variable thickness using first order shear deformation theory (FSDT) and perturbation method, *Chinese Journal of Mechanical Engineering* **28**(6): 1149-1156.
[17] Khoshgoftar M. J., 2018, Second order shear deformation theory for functionally graded axisymmetric thick shell with variable thickness under non-uniform pressure, *Thin-walled Structures Comprise* **144**: 106286.
[18] Omidi M., Loghman A., Arefi M., 2019,The effect of grading index on two-dimensional stress and strain distribution of FG rotating cylinder resting on a friction bed under thermomechanical loading*, Journal of Stress Analysis* **3**(2): 75-82.
[19] Kumari P., Singh A., 2019, *Recent Advances in Structural Engineering,* Springer Singapore.
[20] Lu C. F., Lim C. W., Chen W. Q., 2009, Semi-analytical analysis for multi-directional functionally graded plates: 3-D elasticity solutions, *International Journal for Numerical Methods in Engineering* **79**: 25-44.
[21] Habibi N., Asadi S., Moradikhah R., 2017, Evaluation of SIF in FGM thick-walled cylindrical vessel, *Journal of Stress Analysis* **2**: 2588-2597.
[22] Kardomateas G. A., Phan C. N., 2011, Three-dimensional elasticity solution for sandwich beams/wide plates with orthotropic phases: The negative discriminant case, *Journal of Sandwich Structures and Materials* **13**(6): 641-661.
[23] Jones R. M., 1975, *Mechanics of Composite Materials*,Washington, Scripta Book Co.
[24] Alibeigloo A., Alizadeh M., 2015, Static and free vibration analyses of functionally graded sandwich plates using state space differential quadrature method, *European Journal of Mechanics, A/Solids* **54**: 252-266.
[25] Filippi M., Carrera E., Zenkour A. M., 2014, Static analyses of FGM beams by various theories and finite elements, *Composites Part B: Engineering* **72**: 1-9.